International Journal of Mining Science and Technology 28 (2018) 745–753

Contents lists available at ScienceDirect

International Journal of Mining Science and Technology

journal homepage: www.elsevier.com/locate/ijmst

# A limit equilibrium fracture zone model to investigate seismicity in coal mines

Daniel Malan *, John Napier

*Department of Mining Engineering, Faculty of Engineering, Built Environment and IT, University of Pretoria, Pretoria 0083, South Africa*

ARTICLE INFO

*Article history:*
Received 18 June 2018
Received in revised form 11 July 2018
Accepted 5 August 2018
Available online 3 September 2018

*Keywords:*
Coal bumps
Limit equilibrium model
Mining rate
Seismicity

ABSTRACT

This paper explores possible synergies between techniques used to minimise seismicity in deep South African gold mines and their applicability to control coal bumps. The paper gives a summary of the techniques used in the deep gold mines and a critical appraisal if these are useful in coal mines. The techniques typically include control of mining rate, preconditioning, optimisation of extraction sequences and centralised blasting. Of particular interest to the coal bump problem is an experimental limit equilibrium fracture zone model implemented in a displacement discontinuity code. This was recently developed for the gold mines to enable the interactive analysis of complex tabular mine layout extraction sequences. The model specifically accommodates energy dissipation computations in the developing fracture zone near the edges of these excavations. This allows the released energy to be used as a surrogate measure of ongoing seismic activity and addresses a number of the weaknesses in the traditional usage of this quantity as a criterion for the design of seismically active layouts. This paper investigates the application of the model to a hypothetical coal longwall layout and the specific problem of coal bumps.



## 1. Introduction

Seismicity in coal mines has been studied for many decades and the size of events range from large mining tremors (local magnitude $M_L > 4$) recorded in the Upper Silesia Coal Basin to the localised pillar bursts frequently associated with mining fatalities [1–4]. Although a large volume of research material is available on this topic, further studies are required as emphasised by Zhao and Jiang: "*Statistics showed that bump accidents caused hundreds of fatalities and injuries in the period from 1997 to 2008 in underground coal mines, and coal bumps have already been one of the most dangerous damage occurrences to underground mining safety in China*" [5]. This risk of coal bumps was also emphasised by other workers [6–10].

A study of seismicity and rockbursts in hard rock mines may be of value when investigating the specific problem of coal bursts. The seismicity in the deep South African gold mines has been problematic for more than a century. This is described in detail by Durrheim: "*As early as 1908, damage in a village near Johannesburg led to the appointment of a committee, chaired by the Government Mining Engineer, to 'inquire into and report on the origin and effect of the earth tremors experienced in the village of Ophirton'. The 1908 Ophirton Earth Tremors Committee found that 'under the great weight of the superincumbent mass of rock... the pillars are severely strained; that ultimately they partly give way suddenly, and that this relief of strain produces a vibration in the rock which is transmitted to the surface in the form of a more or less severe tremor or shock'* " [11]. A century later, the seismic problems have not disappeared and Fig. 1 illustrates damage experienced in the face area of a deep gold stope caused by a magnitude 2.0 event.

As indicated in Fig. 1, the small rock fragments are visible on the footwall, and some of the shakedown was caught by the temporary nets used in this area.

Various measures to mitigate the risk to workers caused by this seismicity have been implemented over the last few decades and this has been largely successful as shown in Fig. 2. This illustrates the seismic fatality trends normalised per hours worked for the period from 2003 to 2016. The decreasing trend of rockburst fatalities indicate that at least some success is obtained with these measures and these are discussed briefly in the next section in relation to possible application in coal mines.

Fig. 2 shows the decrease in rockburst fatalities (orange line) from 2003 to 2016 (source: DMR SAMRASS database, courtesy D. Adams).

* Corresponding author.
*E-mail address:* francois.malan@up.ac.za (D. Malan).

https://doi.org/10.1016/j.ijmst.2018.08.003
2095-2686/

**Fig. 1.** An example of minor damage caused by seismicity in a deep gold mine in South Africa.

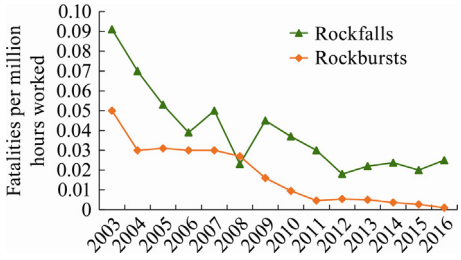


**Fig. 2.** Decrease in rockburst and rock fall fatality rates (fatalities per million hours worked) for all South African mines.

## 2. Methods to mitigate the rockburst risk in deep gold mines and possible application in coal mines

Five key methods are used to mitigate the seismic risk in deep gold mines. These are discussed below with some reference to possible application in coal mines. The five methods are centralised blasting, mining rate, optimising layouts, preconditioning and rockburst resistant support. A further important aspect to manage the seismicity, not discussed in this paper, is the extensive seismic networks and associated data analysis and hazard assessment [12]. These networks are also used in the coal mining industry [13–15]. Readers are referred to these references for additional information.

### 2.1. Centralised blasting

Centralised blasting is a key tool that is used to reduce the exposure of mining personnel to the seismic hazard. The gold mines in South Africa are not mechanised owing to the hard rock and the narrow tabular geometry. Mining is done using a method of hand-held drilling and blasting. Seismic activity is triggered by the blasts and the risk to workers can be mitigated by adopting a centralised blasting policy. A centralised blasting system allows for all blasts within a mine to be synchronized from a dedicated computer on surface, usually from the mine's control room. A typical system consists of a host computer networking with a number of blasting stations to facilitate the arming, priming and firing of electronic or electric detonators. The system increases safety on the mine as all panels are be blasted from a safe location, once all personnel have been evacuated from their working places. The effect on seismicity when implementing centralised blasting is illustrated in Fig. 3. Note that a large proportion of the seismic activity occurs during the so–called "blasting window" when no mining personnel are allowed underground. This technique has no application in mechanised coal mines.

As shown in Fig. 3, this was for data collected in 2015 and 1962 events ranging from M0.0 to M3.7 were recorded and the seismic peak occurs between 18 and 21 h (these hours are indicated by "18" and "21" in Fig. 3 on the x-axis) when the workers are not in the mine.

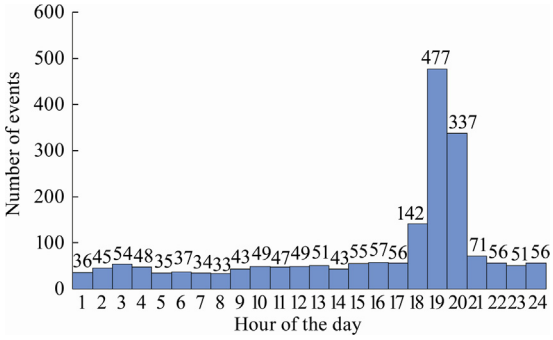


**Fig. 3.** Typical diurnal distribution of seismicity in a gold mine using centralised blasting.

### 2.2. Mining rate

It is known from experience that mining rate has an effect on the levels of seismicity in the deep gold mines of South Africa [16]. This has been disputed by some researchers based on work done by McGarr and Wiebols who postulated that the overall seismic deformation is simply related to mining according to [17]:

$$\sum M_0 = G\Delta V_c \tag{1}$$

where $\sum M_0$ is the summation of all the seismic moments; $G$ the shear modulus of the rock mass; and $\Delta V_c$ the volumetric stope closure due to mining. Based on this work, McGarr and Wiebols stated: "*the number of large tremors per unit volume of rock mined is independent of the rate of mining*" [17].

Cook et al. nevertheless found an increase in the number of rockbursts for a face advance rate of more than 4 m/month for small abutments and 8 m/month for large abutments [18]. Numerical modelling studies of mining rate were conducted by Napier and Malan and Malan [19–21]. For the deep gold mines, it is generally accepted that high stress peaks close to the face may increase the likelihood of strain bursting. A continuum viscoplastic model appeared to be a useful approximation to simulate the time dependent nature of the fracture zone. This model, when applied to mining rate problems, illustrated that high mining rates may lead to higher stress peaks close to the stope face. Similar qualitative results were obtained using a discontinuum viscoplastic model. The fracture zone extent ahead of the mining face decreases for faster mining rates, leading to an increase in the amount of seismic energy released following each mining step. These studies were carried out for plane strain geometries and the effect of volume of mining over a large area with many individual panels was not considered.

Klokow et al. conducted an assessment of dip pillar mining at a Carbon Leader Mine in South Africa [22]. The authors stated that significant changes in the seismic character of a raise line at the mine were observed after production of about 20000 $m^2$ in the particular raise line and when mining spans reached between 100 and 120 m. They also found a significant change in seismic behaviour when the total production at the shaft exceeded 12000 $m^2$/month. Riemer carried out a study of the increase in seismicity at a Carbon Leader Mine [23]. The analysis indicated that this increase appears to be associated with an increased mining rate in a tightly clustered area. His proposal of a "clustering index" indicated that mining rates which exceed approximately 13000 $m^2/km^2$ per month lead to an increased seismic response.

In spite of a lack of quantitative data, a key strategy currently used by geotechnical personnel on some of the mines is to reduce the mining rate when an increase in seismicity is observed. Currently, the "safe" mining rate on the mines is typically determined

on a trial-and-error basis. The unit "$m^2$/month" is typically used as a measure of "volume" of mining as the mined reefs are flat dipping tabular orebodies. The typical mining height varies between 1 and 1.6 m. The area mined during each month can therefore be obtained easily from a plan view of the mine workings. The corresponding volume of rock mined is obtained by multiplying the area mined by the average stoping width. A typical practical measure employed to control the mining rate is to limit the number of mining crews per raise connection.

Regarding mining rate in coal mines, Linkov noted that in the Kizel coal mines, doubling the rate of coal cutting on the face from 0.27 to 0.54 m/min resulted in a drastic increase in the incidence of rockbursting [24]. Nawrocki developed a one-dimensional semi-analytical solution for the time-dependent behavior of a coal seam to investigate the rate of face advance [25]. The analysis indicated that rapid ore extraction produced zones of high stress concentrations close to the longwall face. Iannacchione and Zelanko described a case study in the Beatrice Mine where bumps were recorded on continuous miner sections where rows of chain pillars l5 to 30 m wide were extracted near the gob. As stated by the authors: "*Individual chain pillars are extracted very rapidly, causing loads to shift before the adjacent pillars can redistribute load in a controlled manner.*" Varying the mining rate therefore appears to be a technique that may find application in both hard rock and coal mines to control seismic activity near excavations [26].

### 2.3. Optimising layouts to minimise seismicity

For the gold mines, it was recognised as early as the 1940′s that remnants left by the scattered mining layouts were a cause of seismicity and longwall mining was introduced as a result [27]. The layouts continued to evolve over the decades and further noteworthy aspects were the introduction of strike and dip stabilising pillars as well as bracket pillars to prevent slip on geological structures [28]. The typical design tools used to optimise these layouts are energy release rate (ERR) and excess shear stress (ESS) calculations evaluated using boundary element codes [29]. The key design objective is to minimise high stress concentrations and to minimise the potential for slip on large geological structures. These innovations led to the current deep level gold mines being designed with closely spaced dip pillars and bracket pillars as shown in Fig. 4.

Fig. 4 presents the dip pillars (red areas) and bracket pillars to clamp some of the dykes (dykes indicated by green lines).

Regarding coal mines, Holland and Thomas stated: "*The cure for pillar-line bumps is to recognise areas that can be expected to become highly stressed and to project the mining plan and* operations *to eliminate such areas insofar as possible. If such areas cannot be eliminated, then the mining plan and operations should be projected to avoid the necessity of disturbing these areas before the stresses have been dissipated.*" [1]. The same approach is used in the deep gold mines whereas the layouts are designed to minimise areas of high stress concentration. Wiejacz and Lugowski investigated the effects of geological structures on seismic events at the Wujek coal mine in Katowice, Poland [30]. They concluded that faults can play an important role in the generation of mining induced seismic events. It was suggested that the mines should not run several longwalls parallel to another in a short period of time. Although it is not clear from this paper what alternative sequence should be followed, this is an indication that the layouts and sequencing of panels in coal mines affect seismicity in a similar manner to that experienced in deep gold mines. Section 2.4 (Fig. 6b) gives a further example of modifying layout designs in a coal mine to alleviate the risk of coal bumps.

Osterwald et al. investigated coal bumps related to geological structures in the Sunnyside District, Utah [31]. Harris indicated that the risk of coal bumps becomes elevated in the presence of elevated overburden depth, faults, mining that crosses remnant structures in previously mined seams and sandstone channels that may concentrate stress [7]. These factors are reminiscent of those contributing to rockbursts in deep gold mines and the optimisation of layouts in both commodity types is clearly a requirement to minimise the risk of rockbursts. Iannacchione and Zelanko noted that extraction sequences and mine layouts influence the way stresses are concentrated around mine openings and therefore play a role in bump occurrence [26]. These considerations suggest that routine numerical modelling of coal mine layouts should be conducted, as for deep gold mines, to identify areas where high stress concentrations occur. Examples of innovative layouts in coal mines to redistribute excessive stress concentrations are the thin-pillar method at the Gary No. 2 Mine and pillar-splitting methods at the Olga, Beatrice, and Cottonwood Mines [26].

### 2.4. Preconditioning

Preconditioning is implemented in deep gold mines to minimise the occurrence of strain bursting in stope faces. This type of seismicity occurs when the formation of the fracture zone ahead of the faces is interrupted. Preconditioning comprises the drilling of holes deeper than the normal production rounds (typically twice the length). By using the correct explosive amounts in each hole, ensuring correct tamping and timing of the holes, the formation of the fracture zone can be enhanced. This is illustrated in Fig. 5. Dechelette et al. conducted seismo-acoustic monitoring in a coal longwall with a high rate of face advance of 7–8 m/day [32]. They noted that heavy tremors are typically preceded by a 2 to 3 h seismic-acoustic lull in the strata corresponding to an accumulation of elastic energy that is suddenly released when the heavy tremor occurs. It is postulated that this is similar to the mechanism proposed for face bursting in the hard rock mines where there is

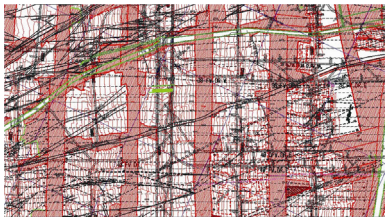

**Fig. 4.** Plan view of a typical modern deep gold mining layout in South Africa.

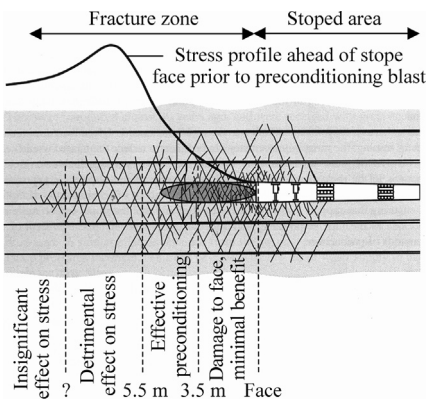


**Fig. 5.** Principle of preconditioning is to mobilise the fracture zone ahead of the stope faces and move the peak stress further ahead of the face [34].

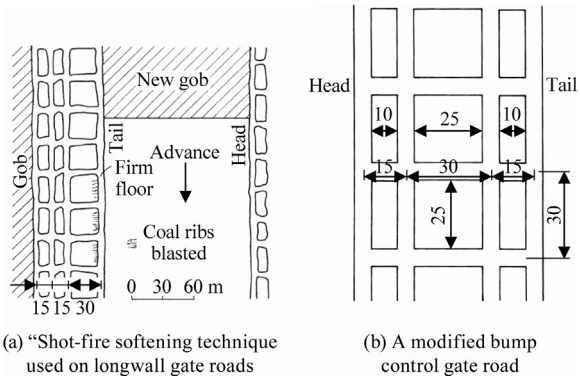


(a) "Shot-fire softening technique used on longwall gate roads (b) A modified bump control gate road

**Fig. 6.** Different techniques used for bump control [4].

a "hang-up" in the formation of the fracture zone resulting in a violent face ejection.

Preconditioning is also used in South Africa in the medium depth hard rock mines where oversized crush pillars occasionally fail violently if they are not fractured using preconditioning. Wu and Zhang describe the use of destress blasting in coal mines where the risk of rockbursts are considered to be high [33].

This technique in coal mines is described by Campoli et al., as the "shot-fire softening" technique [4]. It was used on tail entry longwall gate roads for bump control (Fig. 6a). The pillar design in this mine was also modified as shown in Fig. 6b. It is of interest that no shot fire softening of the narrow pillars adjacent to the tail workings was necessary as they fracture and yield upon approach of the longwall face under abutment-zone loading. The large pillar was required for roof support considerations and was isolated from miners and equipment by the yield pillar. The working area was shielded if the large pillar became overstressed and "bumped". Techniques of de-stressing in coal mines are described by Haramy and McDonnell and one of these is shown in Fig. 7 [35].

### 2.5. Rockburst resistant support

To provide enhanced protection to mining personnel in areas prone to seismicity in the gold mines, consideration is given to the energy absorption capability and area coverage of the support system. This is described in detail in Ryder and Jager [29]. Fig. 8 illustrates the type of support that can be used. Yielding roof bolts are also used in some areas.

As shown in Fig. 8, backfill and yielding steel props can be seen in photograph on the left, and the mines also introduced permanent steel mesh (on the right) in some areas to give better area coverage.

The application of these yielding support units for coal mine applications is discussed in some references. Zhao and Jiang provide photographs of heavy steel arch sets damaged by rockbursts

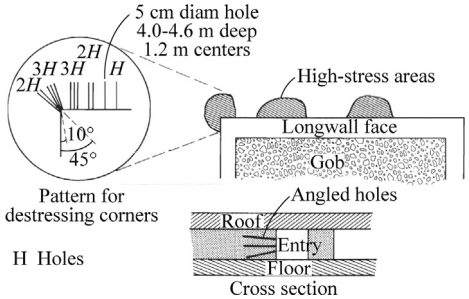


**Fig. 7.** De-stressing technique for a coal longwall face [35].

**Fig. 8.** Examples of support in deep gold mines prone to seismicity.

[5]. Iannacchione and Zelanko describes innovative support strategies being used ranging from yielding leg arches at the Sunnyside Mines to material-filled cribs employed in eastern Kentucky drift mines [26].

## 3. A Limit equilibrium fracture zone model to investigate the effect of mining rate

From the review of techniques used to minimise the risk of seismicity above, it appears that the parameter that is currently poorly understood and which requires further investigation is the effect of mining rate. Only limited work has been carried out on this parameter in relation to coal bumps. A limit equilibrium model implemented in a boundary element computer code has been developed recently to simulate the time dependent nature of the fracture zone in deep gold mines. The sections below explore the application of this model to coal mine studies.

### 3.1. Numerical modelling to investigate coal bumps

Numerous examples can be found in literature describing numerical modelling to investigate coal bumps. The boundary element program, LaModel, is a popular code to simulate coal mine layouts [36]. The incorporation of energy release calculations in LaModel 3.0 allowed for mine layout design in bump prone areas [37]. Wang et al. described the use of energy release calculations in the LaModel code to investigate the risk of bumps in multiple seam longwall mining [38]. Energy release calculations appeared to be useful for this particular application and the technique shows promise. It nevertheless appeared to be unsuccessful regarding coal bump potential in Crandall Canyon Mine in Utah [37].

Alternative computational techniques have also been used to investigate coal bumps. Haramy and McDonnel used a finite element code as well as the MULSUM code to investigate the redistribution of stress when destressing a longwall face [35]. Harris used discrete element modelling (3DEC) to model the behaviour of squat pillars and their potential for violent failure [7]. The section below describes the application of the TEXAN code that was originally developed to simulate the hard rock pillars in the platinum mines of South Africa [39,40].

### 3.2. Overview of the TEXAN code and the incremental stability measure

TEXAN is a displacement discontinuity boundary element code that can solve 2D and 3D problems with multiple interacting tabular reef planes and planar fault planes. These planes are tessellated with displacement discontinuity elements to represent stope ride and elastic convergence movements or to model slip movements on fault planes. Additional facilities exist to allow the sequential activation of discontinuity elements allowing the simulation of fault slip "growth" according to specified growth rules. Elements can be in an "infinite" space or in a "semi-infinite" space with a flat, stress-free surface. In the original

development of the code, the material is assumed to be elastic and isotropic. Analytical kernel expressions are used to compute half-space influence functions in 3D. Bedding planes may be represented by displacement discontinuity elements which have appropriately assigned strength and friction values. The computational analysis of these problems can be extremely arduous and a number of numerical difficulties can arise in modelling the interaction and bending of closely spaced, parallel discontinuities. An alternative approach that has been proposed in past studies is to tailor the displacement discontinuity influence functions to mimic the large-scale movements of bedded strata. One of these representations is the so-called "frictionless laminated model" (abbreviated here to FLM) in which the rock mass is assumed to comprise a stack of contiguous, thin elastic plates [41]. The FLM is used in the computer code LaModel discussed above [36]. In view of the possible utility of the FLM, a special module based on Salamon's formulation has been included in the TEXAN computer program to allow this option for the modelling of horizontally layered strata [41].

The most common criterion that has been used traditionally in the design of deep level mining layout sequencing in South Africa is the so-called energy release rate (ERR) criterion [42,43]. In this criterion, the "energy release" increment, $\Delta W_A$ represents the difference between the incremental work done by gravity forces acting on the rock mass, $\Delta W$, and the incremental change in the strain energy, $\Delta U$, that is stored in or released from the rock mass when the excavation boundary is extended during a mining step [44]. This can be expressed as

$$\Delta W_A = \Delta W - \Delta U \tag{2}$$

In the case of a tabular excavation it is convenient to express the mining step increment in terms of the area mined with respect to the plan view of the excavation shape. If the incremental area mined is designated by $\Delta A$ then the energy release rate is defined to be

$$ERR = \lim_{\Delta A \to 0} \frac{\Delta W_A}{\Delta A} \tag{3}$$

*ERR* values are computed in general layout configurations by using stress analysis programs such as MINSIM based on the displacement discontinuity boundary element method (DDM) [45–47]. In this case, the excavation is approximated as a narrow slit and in many applications the seam or reef material is assumed to be rigid and to have infinite strength. The use of *ERR* as a design criterion to guide layout sequencing and extraction ratios has been discussed at length and has a number of practical shortcomings in providing a measure of mining rockburst hazard [48,49]. The most significant drawback of the *ERR* criterion, used within a purely elastic model of rock deformation, is that no dissipative mechanisms are incorporated into the model to allow for local on-reef face crushing and failure. Eq. (3) represents the local value of the energy release at each point of the tabular excavation boundary and can be used as a measure of the local stress concentration at the stope face. A measure of the stability of excavation enlargement can be obtained by modifying Eq. (2) to include an energy dissipation term $\Delta W_D$. If the dissipation term is appropriately evaluated, a general measure of incremental mining "stability", designated as $\Delta W_R$, can be defined to be:

$$\Delta W_R = \Delta W_A - \Delta W_D \tag{4}$$

The incremental stability measure, defined by Eq. (4), is associated with each incremental change to the excavation shape and may, in addition, include released energy from explicitly modelled faults or fractures. Recently Napier and Malan proposed that the fracture zone adjacent to the edges of tabular excavations can be represented by a simple time-dependent limit equilibrium model [44]. In this case the energy dissipation term $\Delta W_D$ can be computed explicitly in a series of discrete time steps with imposed face advance increments corresponding to a given mining schedule.

### 3.3. Limit equilibrium model of the fracture zone

The time-dependent limit equilibrium model proposed by Napier and Malan provides a representation of the on-reef horizontal and vertical stress distribution adjacent to a mining face [44]. The details of the model are described in study by Heunis and also in Napier and Malan and are not repeated here [16,43]. The limit strength model postulates that if the seam or reef material fails, a specific relationship exists between the seam normal stress $\sigma_n(P,t)$ and the seam parallel stress $\sigma_s(P,t)$ at point $P$ in the unmined excavation plane. The following relationships then applies:

$$\sigma_n(P,t) = \sigma_c(P,t) + m(P,t)\sigma_s(P,t) \tag{5}$$

where the strength envelope parameters $\sigma_c(P,t)$ and $m(P,t)$ are position and time-dependent functions. A drawback of the model is that failure of the material is restricted to the seam or reef plane only. This may nevertheless be a good approximation of coal mine problems where pillar scaling occurs while the roof and floor remains intact (Fig. 9).

The strength envelope given in Eq. (5) is determined by considering the transition between three bounding envelopes as depicted in Fig. 10.

The transition between the initial limit strength and the residual limit strength envelopes is assumed to be governed by a strength decay function $F(\tau)$ that depends on the elapsed time $\tau = t - T(P)$ between the current time $t$ and the initial time of failure, $T(P)$, at point $P$. Specifically, it is postulated that

$$\sigma_c(P,t) = \sigma_c^f + (\sigma_c^0 - \sigma_c^f)F(t - T(P)) \tag{6}$$

and

$$m(P,t) = m_f + (m_0 - m_f)F(t - T(P)), \tag{7}$$

**Fig. 9.** Scaling of a coal pillar in the Vaal Basin in South Africa [50].

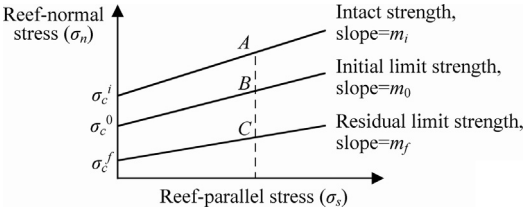


**Fig. 10.** Limit strength envelopes for time-dependent strength decay representation [16].

Where $F(\tau)$ is the decay function. In the present analysis, it is assumed that, $F(\tau) = 1$ if $\tau < 0$ and that $F(\tau)$ is a simple exponential function of the form:

$$F(\tau) = \left(\frac{1}{2}\right)^{\frac{\tau}{\lambda}} = e^{-\alpha\tau} \tag{8}$$

When $\tau \geqslant 0$, $\lambda$ is a half-life parameter and the corresponding exponential decay exponent is $\alpha = \ln(2)/\lambda$. The parameter $\lambda$ effectively defines the problem time scale in terms of proposed mining schedules.

### 3.4. Simulation of longwall mining at different mining rates

As a simple case study, the longwall geometry of coal pillar extraction shown in Fig. 11 was simulated using the TEXAN code. This is based on the approximate dimensions shown in Fig. 6. The size of pillar type A is 25 m × 25 m and pillar type B is 25 m × 10 m. The width of the roadways is 5 m. The host rock was assumed to be sandstone. The parameters used in the models are given in Table 1. This particular geometry was selected as to investigate the effect of mining rate as well as the possible bursting of the pillars in the tail as the longwall face approaches.

Figs. 12 and 13 illustrate some preliminary results when assuming a simple infinite depth model where the host rock is assumed to be isotropic elastic and the seam is allowed to fail according to the limit equilibrium model. No time dependency of the seam failure was allowed in these initial runs. The crushing of the pillar

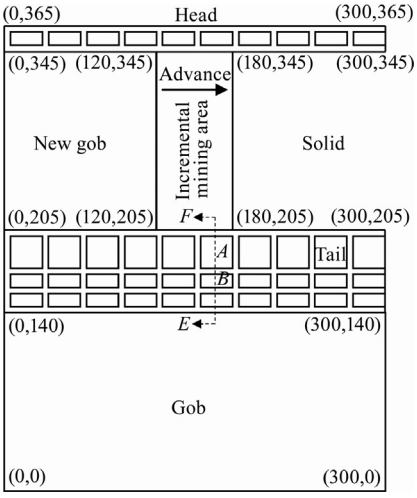


**Fig. 11.** Geometry modelled with the TEXAN code to simulate the longwall mining.

**Table 1**
Parameters used in the simulations.

| Parameter | Value |
|---|---|
| Depth (m) | 400 |
| Mining height (m) | 4 |
| Young's modulus (sandstone) (GPa) | 15 |
| Poisson's ratio (sandstone) | 0.25 |
| Intact seam strength $\sigma_c^i$ (MPa) | 4 |
| Intact seam slope parameter $m_i$ | 4 |
| Initial failed seam strength $\sigma_c^0$ (MPa) | 3 |
| Initial failed seam slope parameter $m_0$ | 3 |
| Residual seam strength $\sigma_c{}^f$ (MPa) | 1 |
| Residual seam slope parameter $m_f$ | 1 |
| Interface friction angle | 20° |
| Half-life parameter $\lambda$ | 20 time units |
| Seam stiffness modulus (MPa/m) | 1346.2 |

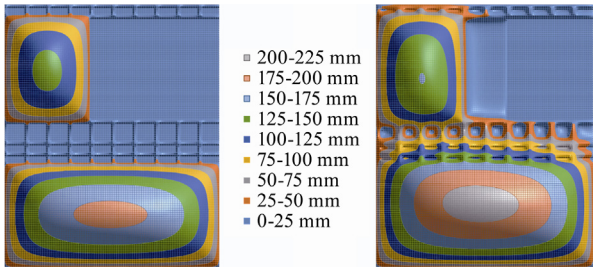


**Fig. 12.** Convergence contours (values in mm) for a model with rigid pillars and a rigid coal seam (left) and for a model where the coal is allowed to crush (right).

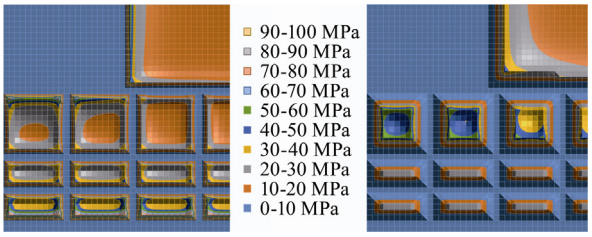


**Fig. 13.** Stress contours (values in MPa) for a model with rigid pillars and a rigid coal seam (left) and for a model where the coal is allowed to crush (right).

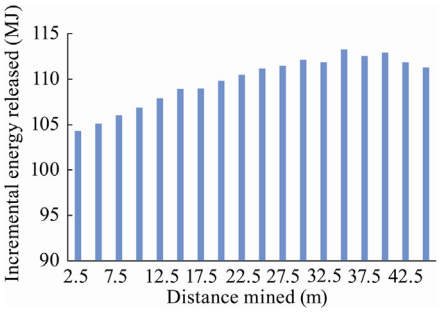


**Fig. 14.** Energy release increments when mining the longwall for a distance of 45 *m*.

edges as a result of assuming the limit equilibrium model is evident in Fig. 12. The extent of fracturing is dependent on the choice of parameters. Fig. 14 illustrates the energy release increments after mining a distance of 45 m.

As noted in Fig. 12, the increase in convergence is visible on the right.

As shown in Fig. 13, the crushing of the small pillars is visible on the right from the reduced stress on the edges of these pillars.

As indicated in Fig. 14, the face was mined using 2.5 m increments per step.

To simulate the effect of mining rate, the longwall face was mined over a distance of 45 m with two simulated advance rates. For the fast mining rate, a 2.5 m increment was mined every 2 time units. In contrast, for the slow mining rate, a 2.5 m increment was mined every 10 time units. For the first simulation, only the coal seam and not the pillars in the gate roads were allowed to crush. The effect of mining rate on the cumulative energy released is shown in Fig. 15. Note that the released energy is much higher for the faster mining rate, indicating a greater hazard in terms of coal bumps. This is in qualitatively agreement with the observations made by Linkov and Iannacchione and Zelanko [24,26]. It should nevertheless be noted that care should be exercised with the interpretation of released energy in complicated geometries

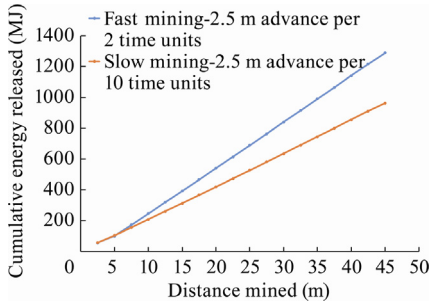


**Fig. 15.** Effect of mining rate on cumulative energy released.

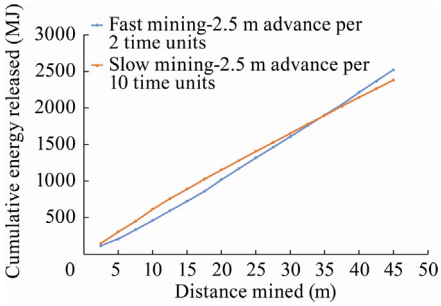


**Fig. 16.** Effect of mining rate on cumulative energy released.

and when crushing in various parts of the model are initiated at different times. Fig. 16 shows again the effect of mining rate, but in this case the pillars in the gate roads were allowed to start crushing during the first time step. The effect of mining rate of the longwall face is now obscured by the crushing of the various pillars in the complex geometry. Figs. 17 and 18 illustrate the

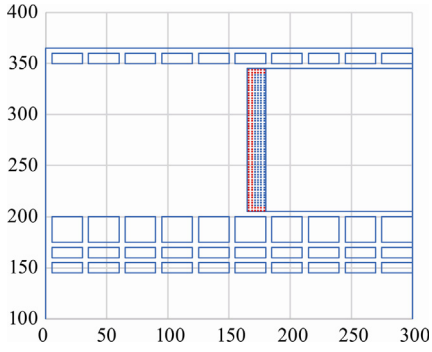

**Fig. 17.** Crushed area of the longwall face is indicated by the red dots.

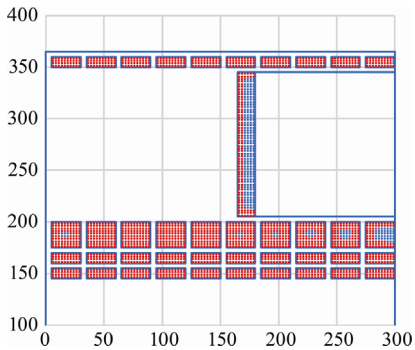

**Fig. 18.** Crushed area of the longwall face and the pillars indicated by the red dots.

crushed zones for the two different models. These results seem encouraging, but further work is now required to calibrate the parameters in Table 1 and to verify the model proposed in Section 3.3.

In Fig. 15, for this simulation, only the coal seam and not the pillars in the head or tail access roadways were allowed to crush (see Fig. 17), and it clearly shows that the slower mining rate results in a smaller release of energy.

In Fig. 16, for this simulation, both the coal seam and the pillars in the head or tail access roadways were allowed to crush (see Fig. 18), and the pillars that start crushing in the first time step make interpretation of the effect of mining rate more difficult.

As shown in Fig. 17, the blue elements are still intact; for this model, the pillars were simulated as rigid pillars and no failure was allowed.

As noted in Fig. 18, the blue elements are intact zones; for this model, the pillars were also allowed to crush.

The model was also investigated in terms of its ability to simulate the effect of the modified bump control gate road as shown in Fig. 6 and described by Campoli et al. [4]. The geometry was modified as shown in Fig. 19 and the large 25 m × 25 m pillar was positioned in the centre of the tail road for this second set of simulations.

As shown in Fig. 19, this geometry is identical in size and pattern to the larger model shown in Fig. 11 except that the 25 m × 25 m pillars are now in the middle of the tail road.

The modelling parameters were again similar to those given in Table 1, except that no time-dependent failure was allowed. The 60 m of face area was mined incrementally for both models and the average pillar stress on pillars A and C was computed. The increase in stress on these two pillars as the face approaches is shown in Fig. 20. Note that the average stress on pillar C is higher than pillar A throughout the incremental mining process. This can probably be ascribed to the fact that pillar D is completely failed increasing the load on pillar C whereas pillar A is still adjacent to the intact seam abutment until the mining face approaches.

When a distance of 60 m has been mined, the face has passed the position of the two pillars.

The result shown in Fig. 20 is dependent on the properties specified in Table 1 and from these results, it is not immediately obvious why the large pillar in the middle of the tail road (pillar C) would be better than one on the side adjacent to the approaching

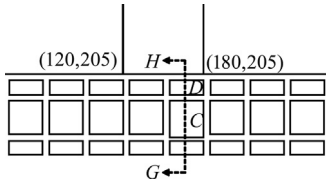


**Fig. 19.** Part of the modified geometry simulated with the TEXAN code.

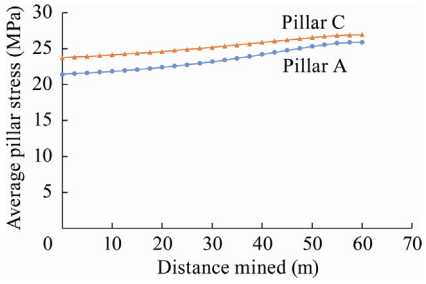


**Fig. 20.** Average pillar stress on pillars A and C as the mining face approaches.

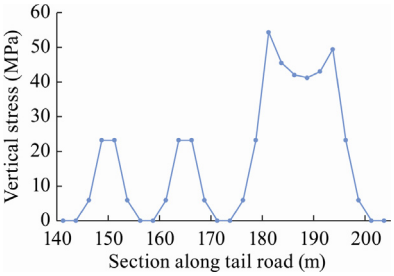


**Fig. 21.** Stress along section EF in Fig. 11.

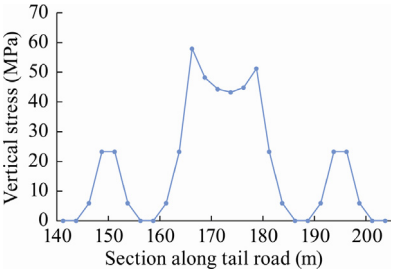


**Fig. 22.** Stress along section GH in Fig. 19.

longwall (pillar A) as suggested by Campoli et al. [4]. This was further investigated by plotting the vertical stress acting on the pillars along sections EF and GH (see Figs. 11 and 19). The stresses along these sections after mining a distance of 60 m are given in Figs. 21 and 22. Note that in both cases the two smaller pillars adjacent to A and C are crushed through and illustrates the typical exponential increase in stress near the pillar edge which is a characteristic of the limit equilibrium model assumption. Although the edges of pillars A and C are failed, the core of both pillars are still intact after the mining face has passed this pillar position.

Further studies with different model parameters will be required to investigate if there are certain stress and strength combinations which imply that it is more favourable to use the geometry in Fig. 19 as compared to Fig. 11. This example again illustrates the need to calibrate the model parameters for site specific conditions.

## 4. Conclusions

This paper explores possible synergies between techniques that are used to minimise hazardous seismic activity in deep South African gold mines and their applicability to control coal bumps. A literature survey indicated that techniques such as preconditioning, optimisation of extraction sequences and rockburst resistant support are used for safe mining in both commodity sectors. A key tool used in the gold mines is centralised blasting and this can unfortunately not be used in many coal operations owing to the mechanised nature of the operations. A parameter that is currently poorly understood and which requires further investigation is the selection of mining rate. Only limited work has been carried out on this parameter in relation to coal bumps and is investigated in this paper.

Of particular interest to the coal bump problem is an experimental limit equilibrium fracture zone model implemented in a displacement discontinuity code. This was developed recently for deep level gold mines to enable the interactive behaviour of complex tabular mine layout extraction sequences to be assessed. The model specifically performs energy dissipation computations in the developing fracture zone near the edges of these excavations. This allows the released energy to be used as a proxy measure of ongoing seismic activity and addresses a number of the weaknesses in the traditional usage of energy release as a criterion for the design of seismically active layouts. The effect of fracture zone strength decay is also incorporated in the model framework. The inclusion of time-dependent behaviour provides the important ability to assess the impact of varying the face advance rate as a strategic option to control extraction stability. It is apparent that no universal design prescription can be applied without a detailed calibration of the characteristic time-decay parameters in the model.

## References

[1] Holland CT, Thomas E. Coal-mine bumps: Some aspects of occurrence, cause and control. United States Department of the Interior, Bureau of Mines; 1954.
[2] Gibowitz SJ. The mechanism of large mining tremors in Poland. In: Proc. 1st Int. Cong. Rockbursts and Seismicity in Mines. Johannesburg; 1984;17-28.
[3] Mutke G, Stec K. Seismicity in the Upper Silesian Coal Basin, Poland: Strong regional seismic events. In: Rockbursts and Seismicity in Mines; 1997; 213–217.
[4] Campoli AA, Kertis CA, Goode CA. Coal mine bumps: Five case studies in the Eastern United States, Information Circular 9149. United States Department of the Interior; 1987.
[5] Zhao YX, Jiang YD. Investigation on the mechanism of coal mine bumps and relating microscopic experiments. In: Proc. 3rd CANUS Rock Mechanics Symposium. Toronto; 2009.
[6] Luo X, Jiang F, Yang S. A trial of microseismic monitoring of coal bumps at an underground coal mine in China. In: RASIM6, Controlling Seismic Risk; 2005;145-147.
[7] Harris KW. Improved Understanding of Coal Pillar Behavior and Bump Potential through the Ground Response Curve, PhD Dissertation. University of Kentucky; 2015.
[8] Iannacchione A, Tadolini S. Occurrence, prediction and control of coalbursts in the US. Int J Rock Min Sci Technol 2016;26(1):39–46.
[9] Hebblewhite B, Galvin J. A review of the geomechanics aspects of a double fatality coal burst at Austar Colliery in NSW, Australia in April 2014. Int J Rock Min Sci Technol 2017;27:3–7.
[10] Zhang C, Canbulat I, Tahmasebinia F, Hebblewhite B. Assessment of energy release mechanisms contributing to coal burst. Int J Rock Min Sci Technol 2017;27:43–7.
[11] Durrheim RJ. Mitigating the risk of rockbursts in the deep hard rock mines of South Africa: 100 years of research. In: Extracting the Science: a century of mining research, Society for Mining, Metallurgy, and Exploration, Inc., Phoenix. Arizona; 2010;156-171.
[12] Mendecki AJ. Keynote Lecture: Principles of monitoring seismic rockmass response to mining. In: Rockbursts and Seismicity in Mines; 1997; 69 – 80.
[13] Gibowitz SJ. The mechanism of large mining tremors in Poland. In: Proc. 1st Int. Cong. Rockbursts and Seismicity in Mines, Johannesburg; 1984;17-28.
[14] Minney D, Kotze G, Van Aswegen G. Seismic monitoring of the caving process above a retreating longwall at New Denmark Colliery, South Africa. In: Rockbursts and Seismicity in Mines; 1997; 125 – 130.
[15] Wu Y, Zhang W. Prevention of rockbursts in coal mines in China. In: Rockbursts and Seismicity in Mines; 1997; 361-365.
[16] Napier JAL, Malan DF. Simulation of tabular mine face advance rates using a simplified fracture zone model. Int J Rock Mech Min Sci 2018;109:105–14.
[17] McGarr A, Wiebols GA. Influence of mine geometry and closure volume on seismicity in a deep-level Mine. Int J Rock Mech Min Sci Geomech Abstr 1977;14:139–45.
[18] Cook NGW, Hoek E, Pretorius JPG, Ortlepp WD, Rock Salamon MDG. Mechanics applied to the study of rockbursts. J.S. Afr Inst Min Metall 1966;66:435–528.
[19] Napier JAL, Malan DF. A viscoplastic discontinuum model of time dependent fracture and seismicity effects in brittle rock. Int J Rock Mech Min Sci Geomech Abstr 1997;34:1075–89.
[20] Malan DF. Time-dependent behaviour of deep level tabular excavations in hard rock. Rock Mech Rock Eng 1999;32(2):123–55.
[21] Malan DF. Implementation of a viscoplastic model in FLAC to investigate rate of mining problems. In: FLAC and Numerical Modelling in Geomechanics, Proc of the Int. FLAC Symp on Num Modelling in Geomech. Minnesota; 1999; 497-504.
[22] Klokow JW, Riemer KL, Ferreira RIL. An initial assessment of the closely spaced dip-pillar mining layout as practiced at Driefontein Gold Mine. In: Proc. ISRM Congress 2003, Technology roadmap for rock mechanics, SAIMM; 2003.
[23] Riemer K. Personal Communication; 2014.
[24] Linkov AM. Rockbursts and the instability of rock masses–Schlumberger Award Lecture. Int J Rock Mech Min Sci Geomech Abstr 1996;33:727–32.
[25] Nawrocki PA. One-dimensional semi-analytical solution for time-dependent behaviour of a seam. Int J Num Anal Meth Geomech 1995;19:59–74.
[26] Iannacchione AT, Zelanko JC. Occurrence and remediation of coal mine bumps: a historical review. In: Proceedings Mechanics and Mitigation of Violent Failure in Coal and Hard-Rock Mines, USBM, Special Publication, SP 01-95; 1995;27-68.

[27] Hill FG. A system of longwall stoping in a deep level mine with special reference to its bearing on the pressure burst and ventilation problems. Association of Mine Managers of the Transvaal. Papers and Discussions; 1942;1:257–276.
[28] Jooste Y, Malan DF. Rock engineering aspects of a modified mining sequence in a dip pillar layout at a deep gold mine. J S Afr Inst Min Metall 2015;115:1097–112.
[29] Ryder JA, Jager AJ. A textbook on rock mechanics for tabular hard rock mines, SIMRAC; 2002.
[30] Wiejacz P, Lugowski A. Effects of geological and mining structures upon mechanism of seismic events at Wujek coal mine, Katowice, Poland. In: Rockbursts and Seismicity in Mines; 1997;27–30.
[31] Osterwald FW, Dunrud CR, Collins DS. Coal Mine Bumps as Related to Geologic Features in the Northern Part of the Sunnyside District, Carbon County, Utah. U.S. Geological Survey professional paper 1514. United States Department of the Interior, Bureau of Mines; 1993.
[32] Dechelette O, Josien JP, Revalor R, Jonis, R. Seismo-acoustic monitoring in an operational longwall face with a high rate of advance. In: Proc. 1st Int. Cong. Rockbursts and Seismicity in Mines, Johannesburg; 1984;83-87.
[33] Wu Y, Zhang W. Prevention of rockbursts in coal mines in China. In: Rockbursts and Seismicity in Mines; 1997;361-365.
[34] Jager AJ, Ryder JA. A handbook on rock engineering practice for tabular hard rock mines. SIMRAC 1999.
[35] Haramy KY, McDonnell JP. Causes and control of coal mine bumps, Report of investigations 9225, United States Department of the Interior; 1988.
[36] Heasley KA. Numerical Modeling of Coal Mines with a Laminated Displacement-Discontinuity Code. PhD dissertation, Colorado School of Mines; 1998.
[37] Sears M, Heasley KA. An application of energy release rate. In: Proceedings of the 28th International Conference on Ground Control in Mining, West Virginia University, Morgantown; 2009.
[38] Wang X, Bai J, Li W, Chen B, Dao VD. Evaluating the coal bump potential for gate road design in multiple-seam longwall mining: a case study. J S Afr Inst Min Metall 2015;115:755–60.
[39] Napier JAL, Malan DF. The computational analysis of shallow depth tabular mining problems. J S Afr Inst Min Metall 2007;107:725–42.
[40] Napier JAL, Malan DF. Numerical computation of average pillar stress and implications for pillar design. J S Afr Inst Min Metall 2011;111:837–46.
[41] Salamon MDG. Deformation of stratified rock masses: a laminated model. J S Afr Inst Min Metall 1991;91:9–25.
[42] Cook NGW. The basic mechanics of rockbursts. J S Afr Inst Min Metall 1963;64:71–81.
[43] Heunis R. The development of rock-burst control strategies for South African gold mines. J S Afr Inst Min Metall 1980;80:139–50.
[44] Napier JAL, Malan DF. A simplified model of local fracture processes to investigate the structural stability and design of large-scale tabular mine layouts. In: 48th US Rock Mechanics / Geomechanics Symposium, Minneapolis, USA; 2014.
[45] Plewman RP, Deist FH, Ortlepp WD. The development and application of a digital computer method for the solution of strata control problems. J S Afr Inst Min Metall 1969;70:33–44.
[46] Deist FH, Georgiadis E, Moris JPE. Computer applications in rock mechanics. J S Afr Inst Min Metall 1972;72:265–72.
[47] Ryder JA, Napier JAL. Error analysis and design of a large-scale tabular mining stress analyser. In: 5th International Conference on Numerical Methods in Geomechanics. Nagoya, Japan; 1985:1549-1555.
[48] Salamon MDG. Energy considerations in rock mechanics: fundamental results. J S Afr Inst Min Metall 1984;84:233–46.
[49] Napier JAL. Energy changes in a rockmass containing multiple discontinuities. J S Afr Inst Min Metall 1991;91:145–57.
[50] Van der Merwe JN, Madden BJ. Rock Engineering for underground coal mining. SIMRAC and SAIMM, SAIMM special publication series 7; 2002.